Journal of Computers Vol. 37 No. 5, October 2026, pp. 241-254
https://doi.org/10.63367/19911599202610370501 5

Uncertain Probabilistic Machine Learning Algorithm for Scene Classification of Humanoid Robot

Shu-Qiong Xu[1*], Cong-Gui Yuan[1], and Shu-Ting Cai[2]

[1] School of Electronic Information, Dongguan Polytechnic,
Dongguan 523808, China
{179444382, 8955504}@qq.com

[2] School of Automation, Guangdong University of Technology,
Guangzhou 510006, China
3357633@qq.com

Received 9 October 2025; Revised 27 January 2026; Accepted 23 February 2026

Abstract. Scene classification has been standing as an important task for many practical applications. In particular, noisy existence, different view angle, variations in lighting conditions, and dynamic backgrounds lead to obstacles in efficient learning and robust classification. Stochastic and uncertain information is always ignored which is existing all time in the practical systems. In this paper, we propose a novel Uncertain Probabilistic Machine Learning Algorithm (UPMLA) for scene classification in humanoid robot system to address these difficulties. Firstly, uncertain probabilistic theorem is integrated with Support Vector Machines to construct Uncertain Probabilistic Fuzzy Support Vector Machines (UPFSVMs) model. Secondly, in order to obtain the solutions of the UPFSVMs, we can transform the probabilistic fuzzy convex optimization problem to the deterministic convex optimization problems. As a result, the solutions of the UPFSVMs can be represented by a set of sub-hyperplanes with the Probabilistic Fuzzy Degree (PDF). Therefore, the optimization problem of the UPFSVMs essentially revolves around designing the PFD. Finally, the design of PFD is predicted on statistical confidence-entropy, which enhance the robustness of the classification process. Compared to other popular scene classification algorithms, experimental results demonstrate the competitiveness of the proposed UPMLA algorithm. Specifically, the UPMLA achieves superior comprehensive metrics within a similar computing budget on the newly built 'Alice' datasets and OT data set.

Keywords: uncertain probabilistic machine learning algorithm, uncertain probabilistic fuzzy support vector machines, uncertain probabilistic theorem, confidence-based probabilistic fuzzy degree

1 Introduction

Scene classification task plays a great role in a wide range of applications and hence has attracted much attention from researchers [1-3]. In recent years, developing various datasets or presenting numerous approaches for scene classification has become an important task in humanoid robots [4-6].

However, a systematic method considering both the various datasets and robust algorithms for scene classification has still not been found [7, 8]. In addition, due to the complexity and variation of scenes, scene classification has also achieved poor performance in humanoid robot systems. Dynamic backgrounds, noisy pollution, diversity of view angles and lighting conditions also increase the degree of difficulty of scene classification in humanoid robot systems [9, 10]. Efficient learning and robust classifying are still challenging hot research topics for humanoid robots.

In recent years, Machine Learning Algorithms (MLAs) [11] have been becoming more and more popular in the application of pattern recognition [12], such as image processing and data analysis [13, 14], with promising results and large potential. Imrie et al. [15] propose a multimodal framework, AutoPrognosis-M, that enables the integration of structured clinical (tabular) data and medical imaging using automated machine learning. AutoPrognosis-M includes 17 imaging models, such as convolution neural networks and vision transformers, along with three unique multimodal fusion techniques. Gui et al. [16] provide a comprehensive review of various SSL approaches, highlighting algorithmic components, application sectors, three primary trends, and outstanding

* Corresponding Author

research issues. A detailed investigation into deep learning strategies for image super-resolution and classification has also been conducted by researchers [17]. Chrysos et al. [18] introduce the first thorough categorization of its applications in deep learning, pinpointing four key domains: higher-order correlation, multi-modal data fusion, dynamic representation modulation, and efficient pairwise operations. Effective deep learning based algorithms are also presented to handle the lesion segmentation, disease prognostic analysis study, and medical image processing [19]. Informative taxonomy based deep learning for image augmentation has been provided with three categories [20]. Even more, digital image analysis based microorganism counting approaches have been studied, followed by trend in development and suggestions for implementing plan.

Many researchers have also paid much attention to the Support Vector Machine (SVM) based scene processing methods [21-23]. Xu et al. [21] proposed an Interval Type-2 Fuzzy Kernel based Support Vector Machine (IT2FK SVM) for scene classification of humanoid robot. A novel three-domain Fuzzy Kernel-based Principal Component Analysis (3DFK-PCA) method is proposed to select the prominent variables and an IT2FM SVM classifier is developed for the comprehensive learning of scene images in complex environment. Zhao et al. [22] introduced a new mmWave radar point cloud classification algorithm, which realized human-vehicle classification employing a newly proposed point cloud feature vector with eleven dimensions and based on kernel support vector machine (SVM) classifier. A new hybrid conditional kernel (HCK) and SVM model based on exponential functions is proposed by Liu et al. [23], and the validity and feasibility of the basic characterizations are introduced theoretically. However, these methods left out the uncertainties and complex of data and robot system, which have not been well discussed in the aforementioned methods. Since statistical theory and fuzzy membership function are powerful to address various uncertainties and the concept of Uncertain Probabilistic Fuzzy Support Vector Machines (UPFSVMs) is not used in the proposed approach. These factors motivate the use of UPFSVMs for the scene classification that is proposed in this paper.

2 Related Works

This section provides concepts and formulas of machine learning algorithm for humanoid robot, and focus on Support Vector Machine (SVM) based classification methods. In addition, stochastic and uncertain information is always ignored which is existing all time in the practical systems. These limitations truly hinder the development of new machine learning-based approaches for image processing. Up to now, efficient learning and robust optimizing is still very difficult to achieve for humanoid robot.

2.1 SVM based Classification Problems

The Convex Optimization Problem (COP) of SVM [21] can be generally defined as in equation (1):

$$\min Q(\varpi, \xi) = \frac{1}{2}\|\varpi\|^2 + \gamma \sum_{j=1}^{N} \xi_j \tag{1}$$

Under the constraint of:

$$\begin{cases} y_j \cdot (\langle \varpi, \phi(x_j) \rangle + b) \geq 1 - \xi_j \\ \xi_j \geq 0, \qquad\qquad j = 1,2,\cdots,N \end{cases} \tag{2}$$

where x_i and y_i denote the feature to be classifying and the corresponding class label of the scene image j. γ denotes the regular parameter, and ξ_j denotes the nonnegative slack variables to deal with permitted errors of the SVM model. b is used to denote the model bias, and $1/\|\varpi\|$ is used to denote the weight vector. $\phi(\cdot)$ is the mapping function, which is used to map the input data from low-dimensional space to the high-dimensional space. With the Vapnik theory, the decision function of the SVM model can be described as follows:

$$D(x) = \text{sgn}(\sum_{SVs} \alpha_j y_j K(x_j, x) + b) \tag{3}$$

where sgn denotes the sign function, $K(\cdot)$ denotes the kernel function for the corresponding mapping function, and *SVs* denotes the support vectors in the SVM model.

SVM approach has been proved to possess the remarkable characteristics of good generalization performance, the absence of local minima, and sparse representation of solution. The performance of SVM depends on the design of kernel functions. This also allows the machine learning researchers to choose the best kernel functions based on specific applications.

2.2 Multiple Feature Kernel (MFK - SVM) based Classification Problems

According to Xu et al. [24], a novel kernel design strategy was proposed to enhance the SVM model's flexibility in capturing the unique features of various learning data. Due to the multiple feature complexity and disturbance of scene images, MFK-SVM based strategy is effective to improve the efficiency of the SVM classification algorithm for humanoid robot. The MFK-SVM strategy for scene classification is defined as follows:

$$K(x, x_j) = c_1 K_1(x, x_j) + c_2 K_2(x, x_j) \tag{4}$$

where c_1 and c_2 are the weighted value for the kernel functions $K_1(\cdot)$ and $K_2(\cdot)$. It can also be described as follows:

$$K(X_i, X_j) = K(K_k(x_{ik}, x_{jk})) \tag{5}$$

where k denotes the number of the kernels in the traditional structure $K(\cdot)$. For example, suppose classification kernel is chosen to be Polynomial kernel, and set $k = 3$, thus the equation (5) can be rewritten:

$$K(X_i, X_j) = (K_1(x_{i1}, x_{j1}) + K_2(x_{i2}, x_{j2}) + K_3(x_{i3}, x_{j3}) + d)^{\eta} \tag{6}$$

2.3 Multiple Domain Kernel (MDK-SVM) based Classification Problems

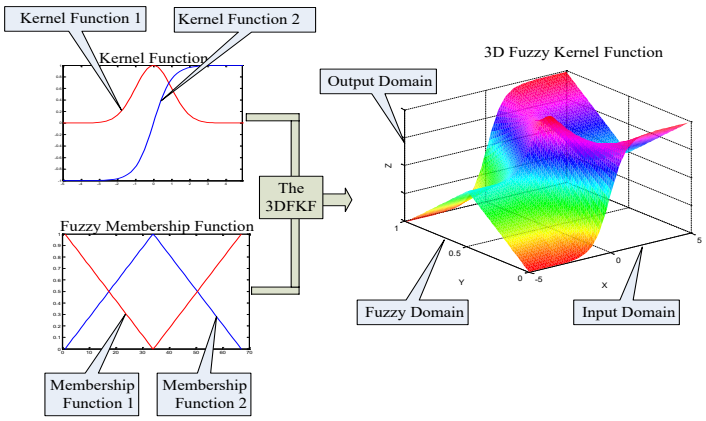


Fig. 1. Mutiple-domain fuzzy kernel function

The research by Xu et al. [25] presented a novel multiple domain fuzzy kernel in the SVM model, which serves as an extension to the standard kernel function, as shown in Fig. 1. Different from the traditional kernel function,

the MDK can be expressed as:

$$\hat{K}(x,z)=\left\{(\frac{K(x,z)}{\mu(K(x,z)})\middle|\forall x,z\in R^{d},\forall K\in\left\{K^{(j)}\right\},j=1,\cdots J\right\} \tag{7}$$

where $K^{(j)}$ is jth element of the traditional kernel functions group. K and J is the element component and the number of the traditional kernel function group, respectively. $\mu(K(x,z))$ is a fuzzy membership function with $0 \leq \mu(K(x,z)) \leq 1$.

3 Uncertain Probabilistic Machine Learning Algorithm for Scene Classification

This section proposes a novel UPMLA for scene classification of humanoid robot. The UPMLA is composed of two parts: the Uncertain Probabilistic Fuzzy Support Vector Machines (UPFSVMs) and the systematic optimization solution. Firstly, the Probabilistic Fuzzy Convex Optimization Problem (PFCOP) of UPFSVMs is defined to describe the probabilistic fuzzy optimization problem in the classification model. Secondly, we can transform the PFCOP in the model UPFSVMs to the deterministic convex optimization problems, therefore the solutions of the UPFSVMs are represented by a set of sub-hyperplanes with the Probabilistic Fuzzy Degree (PFD). Finally, the confidence-based design of PFD is given following the transformation.

3.1 Uncertain Probabilistic Fuzzy Support Vector Machines

We define the Probabilistic Fuzzy Convex Optimization Problem (PFCOP), which is followed by the optimization algorithm. $1/\|\tilde{\varpi}\|$ is a probabilistic fuzzy number which is used to describe the probabilistic fuzzy margin. Giving the data set $\{x_j, y_j\}, j = 1, 2, ..., \tilde{N}$, the PFCOP can be described as:

$$\min Q(\tilde{\varpi},\tilde{\xi})=\frac{1}{2}\|\tilde{\varpi}\|^{2}+\tilde{\gamma}\sum_{j=1}^{\tilde{N}}\tilde{\xi}_{j} \tag{8}$$

Under the constraint of:

$$\begin{cases} y_{j}\cdot(\left\langle\tilde{\varpi},\tilde{\phi}(x_{j})\right\rangle+\tilde{b})\geq 1-\tilde{\xi}_{j} \\ \tilde{\xi}_{j}\geq 0, \qquad\qquad j=1,2,\cdots,\tilde{N} \end{cases} \tag{9}$$

Where $\tilde{\xi}_{j}\in\left\{\frac{\xi_{j}^{1}}{P(\mu^{1})},\frac{\xi_{j}^{2}}{P(\mu^{2})},\cdots\frac{\xi_{j}^{S}}{P(\mu^{S})}\right\}$, $\tilde{b}\in\left\{\frac{b^{1}}{P(\mu^{1})},\frac{b^{2}}{P(\mu^{2})},\cdots\frac{b^{S}}{P(\mu^{S})}\right\}$, $\tilde{\varpi}\in\left\{\frac{\varpi^{1}}{P(\mu^{1})},\frac{\varpi^{2}}{P(\mu^{2})},\cdots\frac{\varpi^{S}}{P(\mu^{S})}\right\}$, $\tilde{\xi}_{j}$, $\tilde{b}$ and $\tilde{\gamma}$ are probabilistic fuzzy parameters in the UPFSVMs with similar definitions in the equations (1) and (2). The Uncertain Probabilistic Fuzzy Kernel (UPFK) in the UPFSVMs would be served as an extension to the MDK. It is difficult to solve the problem described in the equation (8-9). The transformation of the UPFSVMs is given in the following section.

3.2 The Transformation of the UPFSVMs

In order to obtain the solution of the UPFSVMs in the equations (8) and (9), it can be also transformed as shown in Fig. 2. Hence, we can transform the PFCOP in the model UPFSVMs to the deterministic convex optimization problems, and in the final the solutions of the UPFSVMs are represented by a set of sub-hyperplane with the PFD. The design of PFD can be expressed in the following section 3.3.

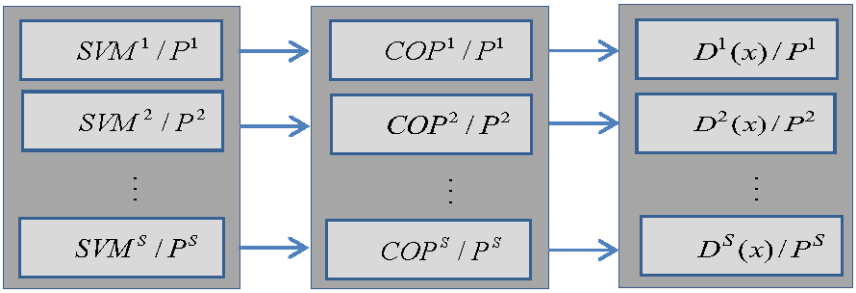


Fig. 2. Transformation of uncertain probabilistic fuzzy support vector machines

The *i*th sub-hyperplane of the UPFSVMs can be expressed by the following equation:

$$D^i(x) = \left(\operatorname{sgn}\left\{ \sum_{j \in SV^i} \alpha_j^i y_j^i \left[K(x_j^i, x) + b^i \right] \right\}, P^i \right) \tag{10}$$

where sgn also denotes the sign function, $K(\cdot)$ denotes the kernel function for the corresponding mapping function, and *SVs* denotes the support vectors in the *i*th SVM model. The probabilistic fuzzy degree P^i of UPFSVMs represents the uncertainties and stochastic information of the samples and robot systems.

We can seen that the UPFSVMs is an extension of the MDK-SVM model. The Uncertain Probabilistic Fuzzy Kernels (UPFKs) would be designed for the UPFSVMs learning, which was also consist of two parts: 1) primary kernel function, and 2) second probability fuzzy degree. The confidence-entropy PFD design is given in the following section.

3.3 The Confidence-entropy PFD Design

From the previous section, suppose we can obtain S sets for the learning of UPFSVMs. In the UPFSVMs, it is very important to find an appropriate design of the PFD for a given humanoid system. For the input variables $\{(X_{pC})_j^i \mid j = 1, 2, ..., J; i = 1, 2, ..., S\}$, the corresponding output values are $\{(y_{pC})_{iw}^i \mid j = 1, 2, ..., J; i = 1, 2, ..., S; w = 1, 2, ..., W\}$. Given the Jth group $\{((X_{pC})_j^i, (y_{pC})_{iw}^i) \mid j = 1, 2, ..., J; i = 1, 2, ..., S; w = 1, 2, ..., W\}$, the mean of output values $(y_{pC})_j^i$ can be calculated:

$$\overline{(y_{pC})_j^i} = \frac{1}{W} \sum_{w=1}^{W} (y_{pC})_{jw}^i \tag{11}$$

For each sample in the *j*th group we calculate its deviation from the mean in the equation (12), where

$$d(y_{pC})_{jw}^i = (y_{pC})_{jw}^i - \overline{(y_{pC})_j^i} \tag{12}$$

Then, the mean variance MV_j^i for each group can be described as followed:

$$MV_j^i = \frac{\sum_{w=1}^{W} (d(y_{pC})_{jw}^i)^2}{W} \tag{13}$$

Thus, the confidence of output values can be calculated as follows:

$$q_{jw}^{i} = 1 - \frac{(d(y_{pC})_{jw}^{i})^{2}}{MV_{j}^{i} \cdot W} \tag{14}$$

For equation (14), it is shown that the value of the confidence of sample is in the interval $0 < q_{jw}^{i} < 1$. Then, we can rewrite the training set as follows:

$$\{((X_{pC})_{j}^{i}, (y_{pC})_{jw}^{i} q_{jw}^{i}) \big| j = 1, 2, \cdots, J;\ i = 1, 2, \cdots, S; w = 1, 2, \cdots, W; 0 < q_{jw}^{i} < 1\} \tag{15}$$

It can be shown that the confidence was related to different importance of each sample for the learning of the optimal hyperplane. The confidence of each clustering sets will be employed to design the fuzzy grade of corresponding membership degree. For the jth group and the ith clustering set, the corresponding membership degree can also be described as follows, respectively:

$$q_{j}^{i} = \frac{\max\limits_{w=1,\cdots,W}(q_{jw}^{i}) - \min\limits_{w=1,\cdots,W}(q_{jw}^{i})}{2} \tag{16}$$

And

$$q^{i} = \frac{\sum_{j=1}^{J} q_{j}^{i}}{J} \tag{17}$$

For the jth group and the ith clustering set, the corresponding information entropy can also be described as follows, respectively:

$$h_{j}^{i} = -\sum_{w=1}^{W} q_{jw}^{i} \log q_{jw}^{i} \tag{18}$$

and

$$h^{i} = -\sum_{j=1}^{J} h_{j}^{i} \log h_{j}^{i} \tag{19}$$

The confidence algorithm is based on the statistical characteristic of samples. It proposed a method to design the membership function in UPFSVMs. According to equations (16) and (17), the membership function of UPFSVMs can be designed as follows:

$$\mu^{i} = \mu(\phi^{i}) = \mu(K^{i}) = q^{i} \tag{20}$$

where $\mu(\phi^{i})$ and $\mu(K^{i})$ is the value of mapping function and kernel function, respectively.

According to equations (18) and (19), the PFD of UPFSVMs can be designed as follows:

$$P^{i} = h^{i} \tag{21}$$

4 Experiments

This section introduces the evaluation metrics, experimental computational steps of the UPMLA, and provides a detailed analysis of the experimental results. Experiments are performed on our own real scenes dataset and

the OT dataset to evaluate the effectiveness of the proposed UPMLA mechanism with different environments. The first experiment is performed on the 'Alice' dataset, which is constructed from Guangdong University of Technology. The second experiment is performed on the OT dataset, which integrated 8 scenes within one large-scale dataset and two small-scale datasets. The performance of the UPMLA mechanism is compared with Long Short Term Memory (LSTM) [26], Capsule Networks (CapsNet) [27], and Vision Transformers (ViTs) [28] classification methods. These classification algorithms are commonly used for performance testing. We can also compare the efficiency of the RBF SVM, WFK-SVM, MDK-SVM and the proposed UPMLA classification methods in terms of calculating Computation Time (CT) on large-scale 'Alice' dataset and the OT dataset. All experiments were conducted on the 'Alice' control platform [21] within MATLAB R2021a.

4.1 Performance Metrics

In this paper, accuracy, precision, and recall [28] are selected as evaluation metrics due to their ability to quantify the dichotomous classification task.

Firstly, Accuracy (Acr) serves as a widely used metric for classification algorithms, evaluating the ratio of correctly predicted samples (TP and TN) to the overall number of samples. The formula for accuracy can be described as follows:

$$Acr = \frac{TP + TN}{TP + TN + FP + FN} \tag{22}$$

where True Positive (*TP*) denotes the number of samples that the classification model correctly predicted as positive classes, True Negative (*TN*) denotes the number of samples that the classification model correctly predicted as negative classes, False Positive (*FP*) denotes the number of samples that the classification model incorrectly predicted as positive classes, and False Negative (*FN*) denotes the number of samples that the classification model incorrectly predicted as negative classes.

Secondly, Precision (Prc) indicates the percentage of samples classified as positive by the model that truly belong to the positive category. The formula for precision can be described as follows:

$$\Pr c = \frac{TP}{TP + FP} \tag{23}$$

Finally, Recall (Rec) is the measure of the proportion of positive class samples that the classification model correctly identifies as positive. The formula for recall can be described as follows:

$$\mathrm{Re} c = \frac{TP}{TP + FN} \tag{24}$$

4.2 Computational Steps of the UPMLA

From the previous section, we have already designed the PFD for the UPMLA, and the computational steps of the UPMLA can be described as follows.

Step 1: PFD design of the UPMLA. The design of the PFD relies on the confidence-entropy with the statistical information. The formulas of detailed calculating steps are provided in equations (11)-(21).

Step 2: Development of Uncertain Probabilistic Fuzzy Kernels (UPFKs). The UPFKs consist of two parts: 1) primary kernel function, and 2) second probability fuzzy degree. The primary kernel functions can be chosen from the traditional kernel functions, such as Linear, Polynomial, and RBF kernels in the UPFSVMs learning. The second probability fuzzy degree can also be set equal to the PFD of the UPMLA.

Step 3: Development of Uncertain Probabilistic Principle Component Analysis (UPPCA). UPPCA also adopts the UPFKs in the analysis process to obtain the classification features from scene images in the uncertain environment for the UPFSVMs classification learning.

Step 4: Optimization of UPFSVMs. The definition of PFCOP is provided in equations (8)-(9). Through the

definition of PFCOP, UPFVSMs aim at minimizing an uncertain bound by maximizing the probabilistic fuzzy margin between the Probabilistic Fuzzy Classify Hyperplane (PFCH) and the training samples.

Step 5: Solution of PFCOP. The solution of PFCOP is represented by a set of sub-hyperplanes with the probabilistic fuzzy degree, and the sub-hyperplanes can be obtained by the transformation as shown in Fig. 2. Fusion operation is applied to obtain the PFCH in equation (10).

4.3 Experimental Results

In this section, experiments are performed on our own real scenes dataset and the OT dataset to evaluate the effectiveness in different environments of the proposed UPMLA mechanism. The control software platform of humanoid robot is designed on the operating system of Windows 10 and developed by Matlab R2021a to understand the scene images. All the algorithms are run independently for 20 times.

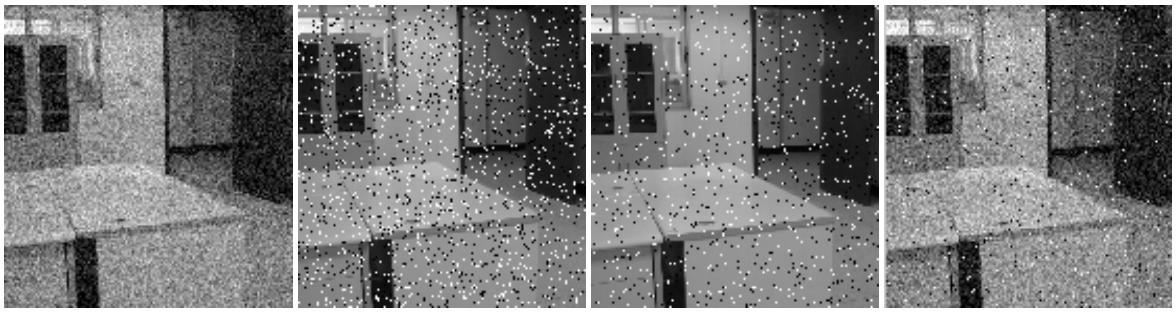
The first experiment is performed on the 'Alice' dataset (four scenes as shown in Fig. 3), which is constructed from Guangdong University of Technology. Scenes are captured under corrupted, different visual angles, and different illumination cases as shown in Fig. 4. 'Alice' datasets are composed of 4000 scene images. Half scenes (images) that are randomly corrupted by different noises, and half scenes (images) that are recorded by different visual angles and different light intensity. We can describe the 'Alice' datasets as follows:

1) Corrupted: images are used for noisy evaluation. In this case, scene image are corrupted by diversity noises, such as impulse noise, Gaussian noise and hybrid noise. scene images for comprehensive noise evaluation are also divided into three small scale datasets: with impulse noise, with Gaussian noise, and 800 with hybrid noise. Some detail noisy scene images can be seen as provided in Fig. 4(a).



(a) Corridor (b) Lab (c) Street (d) Landscape

Fig. 3. 'Alice' datasets are constructed by scenes



(a) In diversity noises



(b) In different visual angles



(c) In different light intensity

Fig. 4. 'Alice' datasets samples

Table 1. Test setting of 'Alice' experiment

Test Scenes	Test parameter	Settings
Corridor Lab Street Landscape	Test metrics	Acr
		Prc
		Rec
	Newly built datasets	Corrupted dataset
		Different view angles dataset
		Different illumination conditions dataset
	Corrupted dataset	Mean 0, variance from 0.005 To 0.05
	Different view angles dataset	From 0 to 180 degree
	Different illumination conditions dataset	Morning
		Noon
		Night
	Running times	20

Table 2. Results of the four algorithms performing on the 'Alice' dataset under hybrid corrupted case

Scenes	Metrics	LSTM	CapsNet	ViTs	The proposed UPMLA
Corridor	Acr	92.9	90.2	93.5	94.5
	Prc	89.5	90.3	91.5	92.4
	Rec	90.2	91.7	92.5	94.8
Lab	Acr	89.0	86.8	89.9	90.6
	Prc	86.8	87.4	91.7	92.5
	Rec	90.4	90.2	90.6	92.4
Street	Acr	88.2	86.5	89.1	91.8
	Prc	80.2	79.9	80.0	86.5
	Rec	84.8	83.6	82.5	88.3
Landscape	Acr	90.5	87.3	90.7	92.5
	Prc	81.7	80.8	84.2	88.5
	Rec	83.9	84.2	85.4	89.2

Table 3. Results of the four algorithms performing on the 'Alice' dataset under different view angles case

Scenes	Metrics	LSTM	CapsNet	ViTs	The proposed UPMLA
Corridor	Acr	89.5	90.5	91.6	92.8
	Prc	85.4	88.2	89.6	90.2
	Rec	86.3	87.7	86.8	91.9
Lab	Acr	90.9	91.6	92.7	93.6
	Prc	86.7	87.9	90.6	94.3
	Rec	88.2	89.5	91.4	92.8
Street	Acr	88.3	88.8	90.3	90.8
	Prc	87.6	86.3	88.9	89.6
	Rec	89.4	88.7	89.5	91.2
Landscape	Acr	87.6	87.9	90.5	90.6
	Prc	86.4	84.2	88.3	91.5
	Rec	86.9	85.7	87.4	89.2

Table 4. Results of the four algorithms performing on the 'Alice' dataset under different illumination case

Scenes	Metrics	LSTM	CapsNet	ViTs	The proposed UPMLA
Corridor	Acr	92.8	90.6	94.0	95.5
	Prc	95.7	94.2	96.6	97.6
	Rec	94.6	93.0	95.8	97.4
Lab	Acr	92.5	88.7	93.8	93.8
	Prc	94.5	95.9	96.8	97.6
	Rec	95.8	94.7	97.4	97.9
Street	Acr	91.7	88.9	92.4	92.8
	Prc	92.5	93.4	93.7	94.5
	Rec	92.8	92.0	93.8	94.6
Landscape	Acr	89.6	88.5	89.6	90.5
	Prc	90.2	90.3	92.3	92.8
	Rec	92.2	91.4	93.5	94.7

Table 5. Results of the four algorithms performing on the OT dataset

Scenes	Metrics	LSTM	CapsNet	ViTs	The proposed UPMLA
Large scale	Acr	91.8	91.6	93.2	94.8
	Prc	92.7	93.4	95.5	96.3
	Rec	94.8	95.1	96.6	97.2
Nature scenes	Acr	92.2	89.7	93.7	94.9
	Prc	94.9	94.6	95.8	97.4
	Rec	95.0	95.1	96.3	97.6
Man-made scenes	Acr	93.7	92.9	93.5	95.1
	Prc	93.5	95.4	95.7	95.9
	Rec	94.8	95.0	95.8	96.8

Table 6. Results of CT calculations for the comparison efficiency of different classification methods

Scenes	CT(s)	RBF-SVM	MFK-SVM	MDK-SVM	The proposed UPMLA
Large scale	Training	1226.24	1227.68	1454.19	1782.51
	Classifying	0.0214	0.0253	0.0217	0.0245
Nature scenes	Training	1152.78	1193.77	1341.36	1874.11
	Classifying	0.0248	0.0261	0.0224	0.0253
Man-made scenes	Training	1108.23	1124.38	1281.72	1994.62
	Classifying	0.0242	0.0254	0.0215	0.0258
Large scale ‘Alice’	Training	1075.63	1094.35	1286.37	1818.25
	Classifying	0.0215	0.0227	0.0201	0.0236

2) Different Visual Angles: 500 scene images are used for different visual angle evaluation. In this case, scene images are mainly captured between and degrees in the horizontal view. Some detail different visual angle scene images can be seen as provided in Fig. 4(b).

3) Different Light Intensity: 1500 scene images are used for different light intensity evaluation. In this case, scene images are captured from visual sensors in different light intensity conditions, including morning, noon, and night. 1500 scene images for different light intensity evaluation can be also divided into three types on the average: weak light, common light, and strong light. Some detail sample different illumination scene images can be seen as provided in Fig. 4(c).

Test setting of ‘Alice’ experiment can be displayed in Table 1, and experimental evaluation results are shown in Table 2 to Table 4. Experimental results can be seen as provided in Table 2, wherein scene images are corrupted by the hybrid noises which include both Gaussian noise (mean 0, and variance from 0.005 to 0.05 randomly) and impulse noise (density from 0.01 to 0.08 randomly). We can see from Table 2, the proposed UPMLA method clearly outperforms other scene classification algorithms. The evaluation results on the ‘Alice’ dataset for different visual angles case and different light intensity cases are also provided in Table 3 and Table 4, respectively. It can be observed from Table 3 to Table 4 that the LSTM, CapsNet, and ViTs classification methods outline similar results, which are inferior to the novel presented UPMLA mechanism in terms of the classification accuracy.

We can also deduce from Table 2 to Table 4 that all classification algorithms perform better on the different light intensity cases than the corrupted and different visual angles cases, because the testing samples are not destroyed much by the different illumination conditions. Due to the structure damage of testing samples, the poor comprehensive performance is presented in the other uncertain cases. To evaluate the robustness performance of the proposed UPMLA mechanism for scene classification of humanoid robot, it is clear that the UPMLA method achieved over 92.5% comprehensive performance indexes in all cases due to its integration of PDF.

The second experiment is performed on the OT data set, which integrates 8 scenes within one large scale data set and two small scale data sets. The large scale data set includes all scenes, in which scenes are classified into 8 categories. The small scale data sets both include 4 scenes (4 natural scenes and 4 man-made scenes, respectively), in which scenes are classified into 8 categories. For the comparison, the parameters settings of

classification algorithms are the same as the previous test. The effectiveness of the proposed UPMLA algorithm is also compared to the LSTM, CapsNet, and ViTs classification methods. All the algorithms are run independently for 20 times. The mean classification metrics of scenes on the large scale (all scenes) and two small scale (natural scenes and man-made scenes) data sets are listed in Table 5. It is observed that the proposed UPMLA approach performs better than the LSTM, Capsule Networks CapsNet, and ViTs classification methods in terms of classification performance described in Table 5. Furthermore, performance metrics are greatly enhanced by incorporating PDF into the UPMLA model for classifier learning.

We can also compare the efficiency of the RBF SVM, WFK-SVM [22], MDK-SVM [23] and the proposed UPMLA classification methods in terms of calculating Computation Time (CT) on large scale 'Alice' dataset and the OT dataset. The large scale 'Alice' dataset is composed of all scenes under the corrupted case, different view angles case, and different illumination case. The average CT of different classification methods under different stages (training and classification) would be shown in Table 6. The RBF SVM, WFK-SVM, and MDK-SVM classification methods also performed better than the UPMLA in the training phase. Note that the training phase is always performed offline. The CT of these different classification methods was also highly similar in the classifying phase. The proposed UPMLA classification method yields over 92.5% comprehensive performance indexes under three small scale 'Alice' datasets, which would provide us with the evidence to use the UPMLA for scene classification.

5 Conclusion

This paper proposes the Uncertain Probabilistic Machine Learning Algorithm for scene classification of humanoid robot. Uncertain probabilistic theorem is integrated with Support Vector Machines to construct Uncertain Probabilistic Fuzzy Support Vector Machines. The solution of UPFSVMs can be represented by a set of sub-hyperplane with the Probabilistic Fuzzy Degree (PDF). Hence, the optimization problem of the UPFSVMs can be transformed to the design of PFD. Finally, the design of PFD relies on the statistical confidence-entropy for classification learning. Compared to the popular scene classification algorithms, UPMLA excels in most cases on accuracy, precision, and recall metrics, demonstrating superior robustness, adaptability, and stability by the newly built 'Alice' datasets and OT dataset. The capability of the proposed UPMLA mechanism for humanoid robots, which can be served for household care, commercial service areas guidance and elderly companionship. Its limitations mainly concentrated in environmental adaptability, computational efficiency, and semantic understanding. In view of these limitations, the future research directions will focus on developing robust multi-modal fusion, integrating natural language processing and human behavior recognition, and promoting the cross-domain migration of classification models.

6 Acknowledgement

The work of Shuqiong Xu was supported by the innovation team of Department of Education of GuangDong Province under Grant No. 2023KCXTD082, and the project for the innovative platform in industry and education integration for higher vocational college of Guangdong Province under Grant No. 2024CJPT027, and the special for key fields of colleges and universities of Guangdong Province under Grant No. 2024ZDZX3120, and the Guangdong Provincial Characteristic and Innovative Project under Grant No. 2025KTSCX375.

References

[1] Z.-Y. Sun, C.-Y. Lui, S.-F. Su, W. Su, Robust Stabilization of High-Order Nonlinear Systems with Unknown Sensitivities and Applications in Humanoid Robot Manipulation, IEEE Transactions on Systems, Man, and Cybernetics: Systems 51(7)(2019) 4409-4416.
https://doi.org/10.1109/TSMC.2019.2931768

[2] B.-H. Yuan, S.-S. Sehra, B. Chiu, Multi-Scale and Multi-Network Deep Feature Fusion for Discriminative Scene Classification of High-Resolution Remote Sensing Images, Remote Sensing 16(21)(2024) 3961.
https://doi.org/10.3390/rs16213961

[3] F. Bi, L. Yang, Research on Acoustic Scene Classification Based on Time–Frequency–Wavelet Fusion Network, Sensors 25(13)(2025) 3930.
https://doi.org/10.3390/s25133930
[4] W.-Y. Hu, C.-J. Lan, T. Chen, S. Liu, L.-R. Yin, L. Wang, Scene Classification of Remote Sensing Image Based on Multi-Path Reconfigurable Neural Network, Land 13(10)(2024) 1718.
https://doi.org/10.3390/land13101718
[5] C. Li, X. Teng, Y. Ding, L. Lan, Instance-Level Scaling and Dynamic Margin-Alignment Knowledge Distillation for Remote Sensing Image Scene Classification, Remote Sensing 16(20)(2024) 3853.
https://doi.org/10.3390/rs16203853
[6] H. Bi, H. Chang, X. Wang, D. Hong, Cross-Attention-Driven Adaptive Graph Relational Network for MultiLabel Remote Sensing Scene Classification, IEEE Transactions on Geoscience and Remote Sensing 62(2024) 1-14.
https://doi.org/10.1109/TGRS.2024.3476089
[7] R.-Z. Hu, Z.-Y. Li, T. Wang, S. Li, Y.-Z. Cai, R. Hu, G.N. Papageorgiou, LCMatch: Layer Cross-Based Semi-Supervised Learning for Remote Sensing Scene Classification, IEEE Transactions on Geoscience and Remote Sensing 63(2025) 4418017.
https://doi.org/10.1109/TGRS.2025.3608572
[8] V.F. Mirama, L.E. Diez, A. Bahillo, V. Quintero, A Survey of Machine Learning in Pedestrian Localization Systems: Applications, Open Issues and Challenges, IEEE Access 9(2021) 120138-120157.
https://doi.org/10.1109/ACCESS.2021.3108073
[9] J. Fan, P. Zheng, S. Li, Vision-based Holistic Scene Understanding Towards Proactive Human–Robot Collaboration, Robotics and Computer-Integrated Manufacturing 75(2022) 102304.
https://doi.org/10.1016/j.rcim.2021.102304
[10] A. Roychoudhury, S. Khorshidi, S. Agrawal, M. Bennewitz, Perception for Humanoid Robots, Current Robotics Reports 4(4)(2023) 127-140.
https://doi.org/10.1007/s43154-023-00107-x
[11] N.A. Shiferaw, Z.L. Mayaluri, P.K. Sahoo, G. Panda, P. Jain, A. Rath, Handwritten Amharic Character Recognition Through Transfer Learning: Integrating CNN Models and Machine Learning Classifiers, IEEE Access 13(2025) 52134-52148.
https://doi.org/10.1109/ACCESS.2025.3553199
[12] S. Abbas, G.A. Sampedro, S. Alsubai, S. Ojo, A.S. Almadhor, A.A. Hejaili, Advancing Healthcare and Elderly Activity Recognition: Active Machine and Deep Learning for Fine- Grained Heterogeneity Activity Recognition, IEEE Access 12(2024) 44949-44959.
https://doi.org/10.1109/ACCESS.2024.3380432
[13] Q. Ling, N.A.M. Isa, Printed Circuit Board Defect Detection Methods Based on Image Processing, Machine Learning and Deep Learning: A Survey, IEEE Access (11)(2023) 15921-15944.
https://doi.org/10.1109/ACCESS.2023.3245093
[14] H. Fan, Q. Li, X. Cao, X. Zhang, B. Chen, H. Xu, T. Zhang, Q. Mao, A Novel Intelligent Fault Diagnosis Method of Helical Gear with Multi-Channel Information Fused Images under Small Samples, Applied Acoustics 228(2025) 110357.
https://doi.org/10.1016/j.apacoust.2024.110357
[15] F. Imrie, S. Denner, L.S. Brunschwig, K. Maier-Hein, M. van der Schaar, Automated Ensemble Multimodal Machine Learning for Healthcare, IEEE Journal of Biomedical and Health Informatics 29(6)(2025) 4213-4226.
https://doi.org/10.1109/JBHI.2025.3530156
[16] J. Gui, T. Chen, J. Zhang, Q. Cao, Z.-N. Sun, H. Luo, D.-C. Tao, A Survey on Self-Supervised Learning: Algorithms, Applications, and Future Trends, IEEE Transactions on Pattern Analysis and Machine Intelligence 46(12)(2024) 9052-9071.
https://doi.org/10.1109/TPAMI.2024.3415112
[17] M. Kapse, N. Elangovan, M. Lalkiya, A. Deshpande, A Comparative Analysis of Machine Learning Algorithms for Image Classification: Evaluating Performance, in: J. Poulose, V. Sharma, C. Maheshkar (Eds.), Data-Driven Decision Making, Palgrave Macmillan, Singapore, 2024 (59-75).
https://doi.org/10.1007/978-981-97-2902-9_3
[18] G.G. Chrysos, Y.-T. Wu, R. Pascanu, P.H.S. Torr, V. Cevher, Hadamard Product in Deep Learning: Introduction, Advances and Challenges, IEEE Transaction on Pattern Analysis and Machine Intelligence 47(8)(2025) 6531-6549.
https://doi.org/10.1109/TPAMI.2025.3560423
[19] S.K. Zhou, H. Greenspan, D. Shen (Eds.), Deep Learning for Medical Image Analysis, Academic Press, 2023.
[20] M. Xu, S. Yoon, A. Fuentes, D.S. Park, A Comprehensive Survey of Image Augmentation Techniques for Deep Learning, Pattern Recognition 137(2023) 109347.
https://doi.org/10.1016/j.patcog.2023.109347
[21] Z. Liu, S.-Q. Xu, Y. Zhang, X. Chen, C.L.P. Chen, Interval type-2 Fuzzy Kernel Based Support Vector Machine Algorithm for Scene Classification of Humanoid Robot, Soft Computing 18(3)(2014) 589-606.
https://doi.org/10.1007/s00500-013-1080-0

[22] Z.-H. Zhao, Y.-Y. Song, F.-C. Cui, J. Zhu, C.-Y. Song, Z.-W. Xu, K. Ding, Point Cloud Features-Based Kernel SVM for Human-Vehicle Classification in Millimeter Wave Radar, IEEE Access (8)(2020) 26012-26021. https://doi.org/10.1109/ACCESS.2020.2970533

[23] S.-W. Liu, Y. Liu, L.-X. Shan, Q.-H. Wang, Y.-H. Sun, L.-S. He, Hybrid Conditional Kernel SVM for Wire Rope Defect Recognition, IEEE Transactions on Industrial Informatics 20(4)(2024) 6234-6244. https://doi.org/10.1109/TII.2023.3344135

[24] Z. Liu, S.-Q. Xu, Y. Zhang, C.L.P. Chen, A Multiple-Feature and Multiple-Kernel Scene Segmentation Algorithm for Humanoid Robot, IEEE Transaction on Cybernetics 44(11)(2014) 2232-2240. https://doi.org/10.1109/TSMC.2013.2297398

[25] Z. Liu, S.-Q. Xu, C.L.P. Chen, Y. Zhang, X. Chen, Y.N. Wang, A Three-Domain Fuzzy Support Vector Regression for Image Denoising and Experimental Studies, IEEE Transactions on Cybernetics 44(4)(2014) 516-525. https://doi.org/10.1109/TSMCC.2013.2258337

[26] N. Sharma, R.K. Sunkaria, A. Kaur, Electrocardiogram Heartbeat Classification Using Machine Learning and Ensemble Convolutional Neural Network-Bidirectional Long Short-Term Memory Technique, IEEE Transactions on Artificial Intelligence 5(6)(2024) 2816-2827. https://doi.org/10.1109/TAI.2023.3324627

[27] H. Dewasurendra, T. Kim, Deep Hybrid Architecture for Very Low-Resolution Image Classification Using Capsule Attention, IEEE Access 12(2024) 141705-141717. https://doi.org/10.1109/ACCESS.2024.3469155

[28] I. Reyes-Amezcua, F. Lopez-Tiro, C. Larose, A. Mendez-Vazquez, G. Ochoa-Ruiz, C. Daul, Vision Transformers for Kidney Stone Image Classification: A Comparative Study with CNNs. <https://arxiv.org/abs/2508.13461>, 2025.